MATHEMATICAL MODELLING OF CANCER INVASION: THE IMPORTANCE OF CELL-CELL ADHESION AND CELL-MATRIX ADHESION

MARK A.J. CHAPLAIN

The SIMBIOS Centre, Division of Mathematics, University of Dundee, 23 Perth Road, Dundee, DD1 4HN, Scotland

chaplain@maths.dundee.ac.uk

MIROSŁAW LACHOWICZ

Institute of Applied Mathematics and Mechanics, Faculty of Mathematics, Informatics and Mechanics, University of Warsaw, ul. Banacha 2, 02-097 Warszawa, Poland

lachowic@mimuw.edu.pl

ZUZANNA SZYMAŃSKA

ICM, University of Warsaw, Pawińskiego 5a, 02-106 Warszawa, Poland

mysz@icm.edu.pl

DARIUSZ WRZOSEK

Institute of Applied Mathematics and Mechanics, Faculty of Mathematics, Informatics and Mechanics, University of Warsaw, ul. Banacha 2, 02-097 Warszawa, Poland

darekw@mimuw.edu.pl

The process of invasion of tissue by cancer cells is crucial for metastasis – the formation of secondary tumours – which is the main cause of mortality in patients with cancer. In the invasion process itself, adhesion, both cell-cell and cell-matrix, plays an extremely important role. In this paper a mathematical model of cancer cell invasion of the extracellular matrix is developed by incorporating cell-cell adhesion as well as cell-matrix adhesion into the model. Considering the interactions between cancer cells, extracellular matrix and matrix degrading enzymes, the model consists of a system of reaction-diffusion partial integro-differential equations, with non-local (integral) terms describing the adhesive interactions between cancer cells and the host tissue, i.e. cell-cell adhesion and cell-matrix adhesion. Having formulated the model, we prove the existence and uniqueness of global in time classical solutions which are uniformly bounded. Then, using computational simulations we investigate the effects of the relative importance of cell-cell adhesion and cell-matrix adhesion on the invasion process. In particular we examine the roles of cell-cell adhesion and cell-matrix adhesion in generating heterogeneous spatio-temporal solutions. Finally, in the discussion section, concluding remarks are made and open problems are indicated.

Keywords: Cancer invasion of tissue; cell-cell adhesion; cell-matrix adhesion; non-local

interactions; existence; uniqueness; boundedness of solutions; computational simulations.

AMS Subject Classification: 35A01, 35A02, 35A23, 35K55, 35K57, 35R09, 35Q92, 65M99, 65N40, 92–08, 92C17, 92C50

1. Introduction

The ability of cancer cells to invade adjacent tissue is a key process in the growth of most cancers. This is a necessary step in the formation of metastases i.e. the spread to distant, secondary locations, distinct from the primary mass. Indeed, metastases (secondary tumours) are responsible for 90% of deaths due to cancer[39]. Although both are highly complex processes, with their genetic and biochemical control mechanisms still not fully understood, at the level of cells and tissues, the two processes of invasion and metastasis are closely linked and have been classified together as one of the so-called "hallmarks of cancer"[21].

Cancer invasion consists of several important steps involving the interplay between the cells themselves and their microenvironment[24]: reduction in or loss of cell-cell adhesion, enhanced cancer cell adhesion to the extracellular matrix, secretion of matrix degrading enzymes leading to extracellular matrix degradation, and the movement or migration of the cancer cells coupled with their proliferation. Cellular adhesion is the binding of one cell to another cell or to a surface or matrix. Cellular adhesion is regulated by specific cell-surface receptors and corresponding adhesion molecules (also known as ligands or counter-receptors) that interact with molecules on the opposing cell or surface. Cancer cells experience both adhesion to themselves i.e. self-adhesion or cell-cell adhesion, and adhesion to components of the extracellular matrix (e.g. collagen, fibronectin, vitronectin) i.e. cell-matrix adhesion.

In general, cell movement through tissue may involve several different mechanisms. However the two most important types of movement for invading cancer cells are diffusion (no preferred direction) and directed motion, with the latter usualy dominating. Directed movement of cancer cells through the extracellular matrix (ECM) is possible due to the breakdown of ECM components, with the cancer cells generally secreting the enzymes which degrade one or more of the ECM constitutive proteins. Through a combination of proliferation and migration the cancer cells then invade and spread into the ECM.

Excellent reviews of cancer growth and development in general and cancer invasion and metastasis in particular can be found in the articles of Hanahan & Weinberg[21] and Friedl & Wolf[16] respectively. A comprehensive description of cancer development, growth and spread may be found in the book of Weinberg[44].

In the last 10-15 years or so, there has been an increasing interest shown in the mathematical modelling of cancer invasion. Previous work in this area may be found in the papers, 1, 2, 8, 10, 11, 17, 18, 23, 30, 31, 32, 38, 40, 41. Many of these models examine the local spread of cancer cells using systems of partial differential equations where the cancer cell migration is governed by diffusion, and the

directed response of the cells to extracellular matrix (ECM) gradients, i.e. haptotaxis. The ECM gradients are created when the ECM is degraded by the matrix degrading enzymes (MDEs) secreted by the cancer cells. As may be expected from such reaction-diffusion-taxis systems, solutions involving an invading front of cancer cells arise and from these one can obtain an indication of the rate of invasion of the cancer cells and the depth of penetration into the ECM. Some papers have adopted a hybrid discrete-continuum approach enabling the tracking of individual cancer cells[1,2]. Other papers have considered an individual-based modelling framework and developed a multi-scale model[33,34] enabling both intracellular dynamics as well as cell-cell interactions to be modelled explicitly.

However, recent work by Gerisch & Chaplain[19] and Sherratt et al.[38] (following the work of Armstrong *et al.*[3]) has considered a cancer cell-cell adhesion term in a continuum model for the first time. These models formulated the problem using non-local integral terms for both cell-cell and cell-matrix adhesion and the concepts of *adhesive flux* and *cell sensing radius*. Being a generalization of reaction-diffusion-taxis systems, these models exhibit qualitatively similar solutions of cancer cell density profiles invading the ECM. However, the introduction of the cell-cell adhesion term had the principal effect of slowing down the invasion rate of the cancer cells. Indeed, for a given value of the cell-matrix adhesion parameter, it was possible to show computationally that a large enough cell-cell adhesion parameter could be chosen so as to localise the cancer and prevent invasion completely (a result also obtained by Sherratt et al.[38]). For certain parameter values, Gerisch & Chaplain[19] also found stationary heterogeneous solutions.

In this paper we adopt the approach of Gerisch & Chaplain[19] and derive a non-local, integro-differential PDE model of cancer invasion describing the spatio-temporal dynamics of cancer cells, extracellular matrix and matrix degrading enzymes. The main aims of the paper are to provide some analytical results concerning the nature of the solutions of such non-local PDE models and to examine computationally the roles of cell-cell and cell-matrix adhesion in some detail. The compuational simulation results show that a range of heterogeneous invasive behaviour can be observed depending on the interplay between the two adhesion parameters, cell-cell and cell-matrix. The structure of the paper is as follows. In the next section we present our mathematical model and make some remarks concerning the non-local terms. In section 4, we prove existence, uniqueness and boundedness of the solutions to our system of equations and then in section 5 we undertake computational simulations of the model to investigate the solution behaviour for a range of parameter values and to examine the relative effects of the key parameters of the model. In the final section concluding remarks are made.

2. The mathematical model

Our model consists of three dependent variables: cancer cell density, c, extracellular matrix density, v, and matrix degrading enzymes, m, and we derive a system of (parabolic) reaction-diffusion-type equations governing the spatio-temporal evolution of these variables. We note that other approaches to modelling such a system are possible, including hyperbolic models[14] and biomechanical models[9]. Indeed adopting a biomechanical approach based on continuum mechanics may even lead to a system of equations which are qualitatively different to that which we propose below[29]. Another alternative approach is to consider individual-based models, which may also take into account the biomechanical properties of cells[33,34].

We assume that the cancer cells migrate into the extracellular matrix through a combination of diffusion and haptotaxis as well as undergoing proliferation. Although it may be more accurate and closer to biological reality to consider nonlinear (degenerate) diffusion[13,36,37,46], for simplicity we assume linear diffusion. For the invasive process that we are modelling here, we believe that diffusion is not a dominant transport term and we have a correspondingly small diffusion coefficient (see Section 4.2 for details). Additionally, we assume that there is also cell-cell adhesion which acts in an opposite manner to the haptotaxis. Following Gerisch and Chaplain[19] we consider non-local interaction terms accounting for both adhesions. Therefore, we start from the following system of integro-differential equations (in non-dimensional form - see section 4):

$$\partial_t c = \underbrace{D_1 \Delta c}_{diffusion} - \underbrace{\nabla \cdot (c\, k_1 \circledast c)}_{cell-cell\ adhesion} - \underbrace{\nabla \cdot (c\, k_2 \circledast v)}_{cell-matrix\ adhesion} + \underbrace{\mu c(1-c-v)}_{proliferation}, \quad (2.1)$$

$$\partial_t v = -\delta v m, \quad (2.2)$$

$$\partial_t m = D_3 \Delta m + \alpha c v - \lambda m, \quad (2.3)$$

where the second and third terms on the right hand side of the equality $(2.1)_1$ define the adhesive fluxes for cell-cell adhesion and cell-matrix adhesion, respectively, i.e.

$$(k_i \circledast u)(x) = \int_\Omega k_i(x,y) u(y)\, \mathrm{d}y, \quad i = 1, 2\,, \quad (2.4)$$

where $\Omega \subset \mathbb{R}^n$, k_i are n–dimensional vectors (kernels), and D_1, μ, δ, D_3, α, λ are positive parameters denoting the cancer cell diffusion coefficient, cancer cell proliferation rate, extracellular matrix degradation rate, matrix degrading enzyme diffusion coefficient, matrix degrading enzyme production rate and matrix degrading enzyme degradation rate, respectively.

The system 2.1 may be written in the following, more general form:

$$\partial_t c = D_1 \Delta c - \nabla \cdot (c G[c\,, v]) + c g_1(c, v)\,, \quad (2.5)$$

$$\partial_t v = -v g_2(m)\,, \quad (2.6)$$

$$\partial_t m = D_3 \Delta m - \lambda m + g_3(v) c\,, \quad (2.7)$$

with a general multicomponent adhesion velocity $G[c\,,v]$ proposed by Gerisch and Chaplain[19]. The function $cg_1(c\,,v)$ describes the rate of cells proliferation. The function $vg_2(m)$ describes the extracellular matrix degradation rate (cf. Sherratt et al.[38] and Gerisch and Chaplain[19]) and the function $cg_3(v)$ describes the rate of enzyme production in response to extracellular-matrix density.

We note that for an appropriate kernel the non-local operator (2.4) approximates the gradient. Indeed, in the case of $\Omega = \mathbb{R}^n$, instead of k (both k_1 and k_2) we set k_ε:

$$k_\varepsilon(x,y) = (y-x)\,\tilde{k}_\varepsilon(|y-x|)\,, \tag{2.8}$$

and for every $0 < \varepsilon < 1$,

$$\operatorname{supp}\tilde{k}_\varepsilon \subset [\,0,\varepsilon\,], \qquad \int_0^\varepsilon r^{n+1}\tilde{k}_\varepsilon(r)\,\mathrm{d}r \int_{\mathbb{S}^{n-1}} |\eta|^2\,\mathrm{d}\eta = 1, \tag{2.9}$$

with

$$\lim_{\varepsilon\to 0}\int_0^\varepsilon r^{n+2}\tilde{k}_\varepsilon(r)\,\mathrm{d}r = 0. \tag{2.10}$$

It is easy to see that such $\tilde{k}_\varepsilon$ can be chosen as a characteristic function supported on $[0,\varepsilon]$. For such a $\tilde{k}_\varepsilon$ one may formally recover the following terms

$$k_\varepsilon \circledast u \longrightarrow \nabla u \quad \text{as} \quad \varepsilon \longrightarrow 0\,. \tag{2.11}$$

In fact, using the Taylor expansion up to the first order, we obtain

$$\begin{aligned}
&(k_\varepsilon \circledast u)(x) = \int_{\mathbb{R}^n} (y-x)\,\tilde{k}_\varepsilon(|y-x|)u(y)\,\mathrm{d}y\\
&= \int_0^\infty \int_{\mathbb{S}^{n-1}} r^n\tilde{k}_\varepsilon(r)u(x+r\eta)\eta\,\mathrm{d}\eta\,\mathrm{d}r\\
&= u(x)\int_0^\infty \int_{\mathbb{S}^{n-1}} r^n\tilde{k}_\varepsilon(r)\eta\,\mathrm{d}\eta\,\mathrm{d}r + \nabla u(x)\int_0^\infty r^{n+1}\tilde{k}_\varepsilon(r)\,\mathrm{d}r \int_{\mathbb{S}^{n-1}} |\eta|^2\,\mathrm{d}\eta\\
&\longrightarrow \nabla u(x)
\end{aligned} \tag{2.12}$$

as $\varepsilon \to 0$.

3. Mathematical analysis

We consider the system (2.5, 2.6, 2.7) in $(0,\infty)\times\Omega$, where Ω is a bounded domain in $\mathbb{R}^n$ with smooth boundary $\partial\Omega$. This system is subject to the boundary conditions

$$\langle \nabla c\,,\nu\rangle = 0 = \langle \nabla m\,,\nu\rangle \quad \text{on} \quad (0,\infty)\times\partial\Omega, \tag{3.1}$$

where ν is the outward normal unit vector field at $\partial\Omega$ supplemented with the condition

$$\langle G[c\,,v]\,,\nu\rangle = 0 \quad \text{on} \quad (0,\infty)\times\partial\Omega. \tag{3.2}$$

Notice that (3.1)-(3.2) ensure no-flux through the boundary $\partial\Omega$ of both cells and enzymes. Our choice of boundary conditions is rather mathematically motivated. In this work we do not consider possible boundary effects. It however may be justified by the fact that the development of the tumour in our case is essentially far from the boundary of the domain containing the tissue. The model is supplemented with initial condition

$$c(0,x) = c_0(x) \geq 0, \;\; v(0,x) = v_0(x) \geq 0, \quad m(0,x) = m_0(x) \geq 0 \;\text{ in }\; \Omega. \tag{3.3}$$

Here, $G[c\,,v]$ is a general non-local mapping modelling the adhesion velocity due to both cell-cell and cell-matrix adhesion. The following assumptions on the function

$$G : C(\bar{\Omega} : \mathbb{R})^2 \mapsto C^{1,\beta}(\bar{\Omega} : \mathbb{R}^n) \quad \beta \in (0\,,1]\,, \tag{3.4}$$

are made:

$$G[c\,,v](x) = \int_\Omega \tilde{G}(x\,,y\,,c(y)\,,v(y))dy \quad \text{for } \; (c\,,v) \in C(\bar{\Omega} : \mathbb{R})^2 \tag{3.5}$$

where $\tilde{G} : \Omega^2 \times \mathbb{R}^2 \mapsto \mathbb{R}^n$ is a continuous function satisfying

$$\tilde{G}(x\,,y,0,0) = 0\,, \quad \text{for all } \; (x\,,y) \in \Omega^2, \tag{3.6}$$

$$\tilde{G}(\,\cdot\,,y,\xi,\eta) \in C^{1,\beta}(\bar{\Omega} : \mathbb{R}^n) \text{ for all } y \in \Omega, (\xi\,,\eta) \in \mathbb{R}^2 \text{ and } \beta \in (0,1). \tag{3.7}$$

There is a constant L_G such that for any $\xi_1\,,\xi_2\,,\eta_1\,,\eta_2 \in \mathbb{R}$

$$\begin{aligned} &|\tilde{G}(x\,,y\,,\xi_1\,,\eta_1) - \tilde{G}(x\,,y\,,\xi_2\,,\eta_2)| + \\ &|\partial_x\tilde{G}(x\,,y\,,\xi_1\,,\eta_1) - \partial_x\tilde{G}(x\,,y\,,\xi_2\,,\eta_2)| \\ &\qquad \leq L_G(|\xi_1 - \xi_2| + |\eta_1 - \eta_2|) \end{aligned} \tag{3.8}$$

uniformly with respect to $(x\,,y) \in \Omega^2$. A natural example of the adhesion velocity which satisfies conditions (3.4)-(3.8) and (3.2) is a functional:

$$\begin{aligned} G[c\,,v](x) = \omega(x)\Big(&\textstyle\int_\Omega (y-x)k_1((|y-x|)c(y)dy + \\ &\textstyle\int_\Omega (y-x)k_2((|y-x|)v(y)dy\Big), \end{aligned} \tag{3.9}$$

where ω is any fixed nonnegative function such that $\omega(x) = 0$ for $x \in \partial\Omega$[19].

We assume that

$$g_1 : \mathbb{R} \times \mathbb{R} \mapsto \mathbb{R} \;\text{ is a locally Lipschitz function} \tag{3.10}$$

and there are $A \geq 0$ and $B > 0$ such that for $c \geq 0$ and $v \geq 0$

$$cg_1(c\,,v) \leq A - Bc\,. \tag{3.11}$$

We assume that

$$g_2\,, g_3 : \mathbb{R} \mapsto \mathbb{R} \;\text{ are locally Lipschitz functions} \tag{3.12}$$

and $g_2(y)\,, g_3(y) \geq 0$ for $y \geq 0$. Moreover we assume that the derivative

$$g_2' \quad \text{exists and it is a locally Lipschitz function.} \tag{3.13}$$

The function $g_1(c\,,v) = \mu(1-c-v)$ with $\mu > 0$ was used in 19 as an example. Functions $g_2(m) = \delta m$ or $g_2(m) = m^2$ and $g_3(v) = \alpha v$ with α as a positive constant are used in 19 and 38.

For further analysis it is convenient to transform system (2.5)-(2.7) to the following

$$\partial_t c - D_1\Delta c + c = -c\Big(\nabla\cdot G[c,v]\Big) - G[c,v]\cdot\nabla c + c\Big(1+g_1(c\,,v)\Big), \tag{3.14}$$

$$\partial_t v = -v g_2(m)\,, \tag{3.15}$$

$$\partial_t m - D_3\Delta m + \lambda m = g_3(v)c\,. \tag{3.16}$$

Next we consider the operators

$$A_1 = -D_1\Delta + I \quad \text{and} \quad A_3 = -D_3\Delta + \lambda I$$

with their realization in the space $X = L^p(\Omega)$. They have a common domain of definition $D = D(A_1) = D(A_3) = \{v \in W^{2,p}(\Omega) : \partial_\nu v|_{\partial\Omega} = 0\}$. Then, since A_1 and A_3 are sectorial operators, fractional powers are well defined and we denote

$$X^\gamma = D(A_1^\gamma) = D(A_3^\gamma) \quad \gamma \in (0\,,1)$$

which is a Banach space equipped with the norm (see 22)

$$\|u\|_{X^\gamma} = \|A^\gamma u\|_X \quad \text{for } u \in X^\gamma\,. \tag{3.17}$$

We shall use the classical semigroup estimates (see 22, p.27)

$$\|A^\gamma e^{-At}u\|_X \le k_\gamma t^{-\gamma} e^{-at}\|u\|_X \tag{3.18}$$

which holds for any $u \in X$ where k_γ and a are positive constants and

$$\|A^\gamma e^{-At}u\|_X \le k_0\|u\|_{X^\gamma} \text{ for } u \in X^\gamma \tag{3.19}$$

where k_0 is a positive constant. We recall also that

$$X^\gamma \subset W^{1,p}(\Omega) \quad \text{for } \gamma > \frac{1}{2}\,, \tag{3.20}$$

$$X^\gamma \subset C^{0\,,r}(\bar\Omega) \quad \text{for } \frac{r}{2} + \frac{n}{2p} < \gamma < \frac{1}{2} + \frac{n}{2p}\,,\ r \in (0\,,1)\,, \tag{3.21}$$

$$X^\gamma = H_p^{2\gamma}(\Omega) \quad \text{for } 0 \le \gamma \le \frac{1}{2} + \frac{1}{2p} \tag{3.22}$$

where $H_p^{2\gamma}(\Omega)$ is the Bessel potential space[42]. We notice also that $H_p^{2\gamma}(\Omega) = F_{p\,,2}^{2\gamma}(\Omega)$ where the latter is the Triebel-Lizorkin space (see 42 Sect. 4.3.1) and that for any $p_0 > p$ the Sobolev space $W^{2,p_0}(\Omega)$ is continuously embedded in the space $F_{p\,,2}^{2\gamma}(\Omega)$ which follows from 43, Sections 3.3.1 and 2.3.5. Notice that for

$$\gamma \in \Big(\frac{1}{2}\,,\frac{1}{2} + \frac{1}{2p}\Big) \quad \text{for } p > n \tag{3.23}$$

(3.20)-(3.22) are satisfied.

Theorem 1. *Suppose that (3.1)-(3.13) and (3.23) are satisfied. If* $c_0, m_0 \in X^\gamma$ *and* $v_0 \in W^{1,p}(\Omega)$ *then there exists a unique global-in-time solution to (2.5)-(2.7)*

with (3.1)-(3.3) such that for any $T > 0$, $c\,, m \in C([0\,, T) : X^\gamma)$ *and* $v \in (C[0, T) : W^{1,p}(\Omega))$. *Moreover,* c *and* m *are classical solutions for* $t > 0$ *and*

$$\sup_{t>0}(\|c(t)\|_\infty + \|v(t)\|_\infty + \|m(t)\|_\infty) < \infty. \tag{3.24}$$

Proof. The existence of a local-in-time solution is based on the Banach contraction theorem. We first denote $E = X \times W^{1,p}(\Omega) \times X$ and for a fixed $T > 0$ which will be specified later we define the space

$$E_T^\gamma = C([0\,, T] : E^\gamma) \quad \text{where } E^\gamma = X^\gamma \times W^{1,p}(\Omega) \times X^\gamma \tag{3.25}$$

equipped with the norm $\|y\|_{E^\gamma} = \max\{\|y_1\|_{X^\gamma}\,, \|y_2\|_{W^{1,p}(\Omega)}\,, \|y_3\|_{X^\gamma}\}$ for $y = (y_1\,, y_2\,, y_3) \in E^\gamma$. Notice that due to (3.8), (3.12) and the embedding (3.21) with (3.20) the terms on the right hand side of (3.14)-(3.16) define mapping $F : E^\gamma \mapsto E$, $F = (F_1\,, F_2\,, F_3)$. In light of (3.12) and (3.20) and the property of the superposition operator acting on the space $W^{1,p}(\Omega)$ for $p > n$ (see 35 Sect. 5.2.3), $m \in W^{1,p}(\Omega)$ and the value of the function $m \mapsto g_2(m)$ is also in $W^{1,p}(\Omega)$. Since the latter space for $p > n$ is an algebra with pointwise multiplication we deduce that the function $(v\,, m) \mapsto F_2 = vg_2(m)$ is also $W^{1,p}(\Omega)$-valued. The hypotheses (3.8), (3.10) and (3.12) with (3.13) as well as the embeddings (3.21), (3.20) imply also that F is a locally Lipschitz function. We note at this point that Lipschitz continuity of the derivative g_2' in (3.13) is necessary for Lipschitz continuity of F_2. Indeed, for any (v_i, m_i) such that $(c_i\,, v_i\,, m_i)$ belongs to a closed ball $B(0\,, \varrho) \subset E^\gamma$, $i = 1\,, 2$ we obtain (after standard computations) that

$$\begin{array}{l} \|F_2(v_1\,, m_1) - F_2(v_2\,, m_2)\|_{W^{1,p}(\Omega)} \leq \\ K_\varrho\left(\|m_1 - m_2\|_{X^\gamma} + \|v_1 - v_2\|_{W^{1,p}(\Omega)}\right) \end{array} \tag{3.26}$$

where K_ϱ depends on ϱ and on $\|g_2'\|_{W^{1\,,\infty}(0\,,U)}$ with $U > 0$ depending on ϱ.

Next we define mapping $\Phi : E_T^\gamma \mapsto E_T^\gamma\,, \Phi = (\Phi_1\,, \Phi_2\,, \Phi_3)\,,$

$$\Phi[c\,, v\,, m](t) = \begin{cases} \Phi_1 = e^{-A_1 t}c_0 + \int_0^t e^{-A_c(t-s)}F_1(c(s), v(s))ds \\ \Phi_2 = v_0 + \int_0^t F_2(m(s)\, v(s))ds \\ \Phi_3 = e^{-A_3 t}m_0 + \int_0^t e^{-A_m(t-s)}F_3(c(s)\,, v(s))ds. \end{cases} \tag{3.27}$$

We note that

$$t \mapsto v_0 - \int_0^t v(s)g_2(m(s))ds \tag{3.28}$$

belongs to the space $C([0\,, T] : W^{1,p}(\Omega))$.

Denoting $y_0 = (c_0\,, v_0\,, m_0) \in E^\gamma$ we take $R > 0$ big enough such that $\max\{\|c_0\|_{X^\gamma}\,, \|m_0\|_{X^\gamma}\} < \frac{R}{2k_0}$ where k_0 has been defined in (3.19) and $\|v_0\|_{W^{1,p}(\Omega)} < \frac{R}{2}$. Next we define $V_T \subset E_T^\gamma$

$$V_T = \{y \in E_T^\gamma : \|y\|_{E_T^\gamma} \leq R\}\,. \tag{3.29}$$

It follows that there exists M_R such that $\sup_{y\in V_T}\|F(y)\|_E < M_R$. We shall show that for T small enough Φ maps V_T into itself. Indeed using (3.18) and (3.19)

$$\|\Phi_1[c\,,v](t)\|_{X^\gamma} = \|A_c^\gamma e^{-A_c t}c_0 + \int_0^t A_c^\gamma e^{-A_c(t-s)}F_1(c(s)\,,v(s))ds\|_X \tag{3.30}$$
$$\leq k_0\|c_0\|_{X^\gamma} + M_R\int_0^T \frac{k_\gamma}{t^\gamma}e^{-as}ds \leq \frac{R}{2} + M_R\frac{k_\gamma}{1-\gamma}T^{1-\gamma}\,.$$

Similar arguments yield

$$\|\Phi_3[c\,,v](t)\|_{X^\gamma} \leq \frac{R}{2} + M_R\frac{k_\gamma}{1-\gamma}T^{1-\gamma} \tag{3.31}$$

and finally

$$\|\Phi_2[v\,,m](t)\|_{W^{1,p}(\Omega)} \leq \frac{R}{2} + TM_RK_R\,. \tag{3.32}$$

We then conclude choosing T such that

$$\max\{TM_RK_R\,, M_R\frac{k_\gamma}{1-\gamma}T^{1-\gamma}\} < \frac{R}{2}\,. \tag{3.33}$$

Similar estimates (cf. 22 p. 55) made for the differences of arguments lead to the conclusion that for T small enough Φ is a contraction and by the Banach theorem it has a fixed point in V_T. Observe now that due to (3.21) for any $T' < T$ function $v : [0\,,T'] \mapsto C(\Omega)$ given by (3.28) is locally Lipschitz. Therefore function $t \mapsto F_1(\cdot\,, v(t))$ in

$$c(t) = e^{-A_1 t}c_0 + \int_0^t e^{-A_1(t-s)}F_1(c(s)\,,v(s))ds,$$

is also a locally Lipschitz X-valued function of time. It then follows from 22 (Sec. 3.3) that there is a maximal time of existence T_{max} of a regular solution $c \in C[0\,,T_{max} : X^\gamma)$ such that for $t \in (0\,,T_{max})\,, c(t) \in D(A_1)$ and by 22 (Sec. 3.5) $c \in C^\beta(0\,,T_{max} : X^\alpha)$ for some $\alpha\,,\beta \in (0\,,1)$. Notice also that $v \in W^{1\,,\infty}(0\,,T : W^{1,p}(\Omega))$. Thus (3.14) is satisfied in a pointwise manner on $(0\,,T_{max})\times\Omega$ and it follows from (3.7) and (3.21) and the regularity theory of parabolic equations that c is in fact the classical solution to (3.14). The same conclusion can be drawn for m.

Let $\tilde{c} = c_1 - c_2\,, \tilde{v} = v_1 - v_2\,, \tilde{m} = m_1 - m_2$ denote the differences of components of any two solutions starting from the same initial condition. The following inequality is an easy consequence of the Lipschitz continuity of all nonlinear terms and the fact that the components of the solutions are L^∞-bounded functions on bounded time intervals

$$\begin{aligned}&\tfrac{d}{dt}\textstyle\int_\Omega(\tilde{c}^2(t,x) + \tilde{v}^2(t,x) + \tilde{m}^2(t,x))dx \leq \\ &Const.\textstyle\int_\Omega(\tilde{c}^2(t,x) + \tilde{v}^2(t,x) + \tilde{m}^2(t,x))dx \;\text{ for }\; t \in [0\,,T_{max}).\end{aligned} \tag{3.34}$$

Now the uniqueness of the solution follows from Gronwall's Lemma.

Next we infer from the maximum principle that $c \geq 0$ on $[0\,, T_{max}) \times \Omega$. Notice that v may be expressed in the form

$$v(t) = v_0 \exp\left\{ - \int_0^t g_2(m(s))ds \right\}, \tag{3.35}$$

and thus it is a nonnegative function. Now it follows from (2.7) that also $m \geq 0$ by the maximum principle.

In order to prove that the solution is global in time i.e. $T_{max} = \infty$ we come back to the divergence form in the first equation (2.5) and integrate it on Ω. Using (3.1), (3.2) and then (3.11) we obtain for $t \in [0\,, T_{max})$

$$\frac{d}{dt}\int_\Omega c(t,x)dx = \int_\Omega c g_1(c,v)(t\,,x)dx \leq A|\Omega| - B\int_\Omega c(t,x)dx\,.$$

Hence, by Gronwall's Lemma we infer that

$$\sup_{t\in[0\,,T_{max})} \|c(t\,,\cdot)\|_{L^1(\Omega)} \leq \max\left\{ \frac{A|\Omega|}{B}\,, \|c_0\|_{L^1(\Omega)} \right\} := K_c\,. \tag{3.36}$$

Since

$$\sup_{t\in[0\,,T_{max})} \|v(t,\cdot)\|_\infty \leq \|v_0\|_\infty \tag{3.37}$$

it follows from (2.7) that

$$\frac{d}{dt}\int_\Omega m(t,x)dx + \lambda\int_\Omega c(t,x)dx = \int_\Omega g_2(v)c dx \leq \sup_{v\in[0\,,\|v_0\|_\infty]} g_2(v)K_c \tag{3.38}$$

and by the Gronwall lemma

$$\begin{array}{l} \sup_{t\in[0\,,T_{max})} \|m(t\,,\cdot)\|_{L^1(\Omega)} \leq \\ \max\left\{ \frac{\sup_{v\in[0\,,\|v_0\|_\infty]} g_2(v)K_c}{\lambda}\,, \|m_0\|_{L^1(\Omega)} \right\} := K_m\,. \end{array} \tag{3.39}$$

It then follows from (3.5)-(3.8) that for all $t \in [0\,, T_{max})$

$$\begin{array}{rl} \|(\sum_{i=1}^n \partial_{x_i} G[c\,,v]) + G[c\,,v]\|_\infty \leq & L_G(\|c(t)|_{L^1(\Omega)}) + \|v(t)|_{L^1(\Omega)} \\ & \leq L_G(K_c + \|v_0\|_\infty|\Omega|). \end{array} \tag{3.40}$$

Next we consider the elliptic operator (3.14) which can be rewritten in the following form

$$-\Delta c + \sum_{i=1}^n b_i \partial_{x_i} c + dc$$

where $b_i = G_i[c,v]$ and $d = \sum_{i=1}^n \partial_{x_i} G[c\,,v])$ are evaluated on the solution. It follows from (3.40) that b_i and d are uniformly bounded on $(0,\infty)\times\Omega$. Since the reaction part is dissipative in the sense of 12, it is possible to use the Moser-Alikakos method (see 12 Sec. 9.3 in our particular case) and derive for c a uniform in time L^∞-bound

from the uniform in time L^1-bound (see 3.36). The same can be done for m. Hence, taking into account (3.35) there is a constant K_∞ such that

$$\sup_{t\in[0\,,T_{max})}(\|c(t)\|_\infty+\|v(t)\|_\infty+\|m(t)\|_\infty)<K_\infty\,. \tag{3.41}$$

This result can be used to show that

$$\|F_1(c(t)\,,v(t))\|_X\le K_1(1+\|c(t)\|_{X^\gamma})\quad\text{for }\ t\in[0\,,T_{max}) \tag{3.42}$$

and

$$\|F_3(c(t)\,,v(t))\|_X\le K_3\quad\text{for }\ t\in[0\,,T_{max}), \tag{3.43}$$

where $K_1\,,K_3$ are constants depending on K_∞. Suppose now that $T_{max}<\infty$ and

$$\max\{\|c(t)\|_{X^\gamma}\,,\|m(t)\|_{X^\gamma}\,,\|v(t)\|_{W^{1,p}(\Omega)}\}\to\infty\ \text{ as }\ t\to T_{max}\,. \tag{3.44}$$

It then follows from 22 Cor. 3.3.5 that

$$\sup_{t\in[0\,,T_{max})}\|c(t)\|_{X^\gamma}+\|m(t)\|_{X^\gamma}<\infty. \tag{3.45}$$

On the other hand (3.20) implies that there is a constant K_m such that $\sup_{t\in[0\,,T_{max})}\|m(t)\|_{W^{1,p}(\Omega)}<K_m$. By (3.35) we obtain

$$\begin{aligned}&\nabla v(t)=\nabla v_0\exp\Big\{-\textstyle\int_0^t g_2(m(s)ds\Big\}\\&-v_0\exp\Big\{-\textstyle\int_0^t g_2(m(s))ds\Big\}\int_0^t g_2'(m(s))\,\nabla m(s)ds,\end{aligned}$$

whence,

$$\sup_{t\in[0\,,T_{max})}\|v(t)\|_{W^{1,p}(\Omega)}\le K_2(\|v_0\|_{W^{1,p}(\Omega)}+T_{max}\sup_{t\in[0\,,T_{max})}\|m(t)\|_{W^{1,p}(\Omega)})<\infty\,.$$

where K_2 is a constant depending on K_∞ and on $\|g_2(\cdot)\|_{W^{1,\infty}(0\,,U)}$ with $U=\sup_{t\in[0,T_{max})}\|m(t)\|_\infty$. This bound along with (3.45) contradicts (3.44). Thus the solution may by prolonged for all $t>0$ and $T_{max}=\infty$. □

4. Computational results: Numerical simulations in 1D

4.1. *Nondimensionalisation*

In this section numerical simulations of the non-local invasion model in the one-dimensional case are presented. Recall the system (2.1):

$$\partial_t c=D_1\partial_x^2 c-\partial_x\cdot(c\,G[c\,,v])+\mu c(1-c/c^0-v/v^0)\,, \tag{4.1}$$

$$\partial_t v=-\delta v m\,, \tag{4.2}$$

$$\partial_t m=D_3\partial_x^2 m+\alpha c v-\lambda m\,, \tag{4.3}$$

where for the cancer cells we have assumed a logistic proliferation function (including competition for space) with proliferation rate μ, a reference tumour density c^0 and extracellular matrix density v^0. $G[c\,,v]$ is the general multicomponent adhesion

velocity proposed by Gerisch and Chaplain[19]. The extracellular matrix is degraded at rate δ upon contact with the degrading enzymes; these are produced at rate α when the cancer cells come into contact with the matrix and decay with rate λ.

In order to solve our system of equations (4.1)-(4.3) numerically we first of all non-dimensionalise the equations. The variables and parameters in the system (4.1)-(4.3) and their associated boundary and initial conditions are transformed into dimensionless quantities using the following reference variables:

i) a reference length scale, L, (*e.g.* the maximum invasion distance of the cancer cells at this early stage of invasion $0.1 - 1cm$);
ii) a reference time unit, $\tau = \dfrac{L^2}{D}$, where D is a reference chemical diffusion coefficient *e.g.* $10^{-6}cm^2s^{-1}$ (see Ref. 5), therefore, we deduce that τ varies between $10^4 - 10^6 sec$;
iii) a reference tumour cell density c^0, extracellular matrix density v^0 and matrix degrading enzymes density m^0 (where $c^0 = 6.7 \times 10^7$ cell cm^{-3}, $v^0 = 10^{-1}$nM and m^0 is an appropriate MDE reference concentration, (see Gerisch & Chaplain[19] for details).

We define the non-dimensional variables:

$$\tilde{t} = \frac{t}{\tau}, \tilde{x} = \frac{x}{L}, \tilde{c} = \frac{c}{c^0}, \tilde{v} = \frac{v}{v^0}, \tilde{m} = \frac{m}{m^0}, \tag{4.4}$$

and new parameters via the following scaling:

$$\tilde{D}_1 = \frac{D_1}{D}, \ \tilde{D}_3 = \frac{D_3}{D}, \ \tilde{\mu} = \mu\tau, \ \tilde{\delta} = \delta v^0 \tau, \ \tilde{\alpha} = \frac{\alpha c^0 v^0 \tau}{m^0}, \ \tilde{\lambda} = \lambda\tau.$$

Henceforth we omit the tildes for notational simplicity, so our non-dimensionalised system reads as follows:

$$\partial_t c = D_1 \partial_x^2 c - \partial_x \left(c\, G[c\,, v] \right) + \mu c(1 - c - v)\,, \tag{4.5}$$

$$\partial_t v = -\delta v m\,, \tag{4.6}$$

$$\partial_t m = D_3 \partial_x^2 m + \alpha c v - \lambda m\,. \tag{4.7}$$

Following Gerisch and Chaplain[19] (see the change of variables in (2.12)), we take the adhesion velocity $G[c\,, v]$ to be:

$$G[c, v](t, x) = \frac{1}{R} \int_0^R \sum_{k=0}^{1} \eta(k) g(c(t, x + \eta(k)r), v(t, x + \eta(k)r)) \omega(r) dr$$

where $\eta(k) = (-1)^k$, $k = 0, 1$ is the right and left unit outer normal, R is the so-called *sensing radius*, $g(c, v)$ is a function representing cell-cell and cell-matrix interaction and ω is a function describing how strong the adhesion velocity is influenced by points of the sensing region at x depending on their distance r from

x. This function should, however, not alter the magnitude of the adhesion velocity. For this reason we require that ω is normalised in the sense that its integral over the sensing region is unity. Hence, we take

$$\omega(r) = \frac{1}{R}\Big(1 - \frac{r}{R}\Big).$$

We note that with the above choice of the function ω, the corresponding kernels k_1 and k_2 are discontinuous (cf. Armstrong et al.[3], Gerisch & Chaplain[19]). The mathematical analysis of the previous section assumed a smooth kernel and therefore is appropriate for the smooth regularization of ω.
Finally, taking $g[c, v] = S_{11}c + S_{12}v$, where S_{11} is the cell-cell adhesion coefficient and S_{12} is the cell-matrix adhesion coefficient, we have our full non-dimensional system of equations:

$$\partial_t c = D_1\partial_x^2 c - \underbrace{\partial_x\Big(\frac{c}{R}\int_0^R \sum_{k=0}^{1} \eta(k) S_{11} c(t, x + \eta(k)r)\,\omega(r)dr\Big)}_{cell-cell\ adhesion}$$

$$\underbrace{- \partial_x\Big(\frac{c}{R}\int_0^R \sum_{k=0}^{1} \eta(k) S_{12} v(t, x + \eta(k)r)\,\omega(r)dr\Big)}_{cell-matrix\ adhesion} + \mu c(1 - c - v) \quad (4.8)$$

$$\partial_t v = -\delta v m \quad (4.9)$$

$$\partial_t m = D_3\partial_x^2 m + \alpha c v - \lambda m. \quad (4.10)$$

4.2. *Parameter values*

We took our baseline set of parameters in line with previous comparable models of cancer cell invasion[1,10,11,19] and whenever possible parameter values are estimated from available experimental data e.g. estimates for cancer cell random motility vary between $10^{-10}\text{cm}^2\text{s}^{-1} - 10^{-9}\text{cm}^2\text{s}^{-1}$ and those for MDE diffusion between $10^{-10}\text{cm}^2\text{s}^{-1} - 10^{-9}\text{cm}^2\text{s}^{-1}$, meaning our non-dimensional parameters D_1 and D_3 are between $10^{-4} - 10^{-3}$ and $10^{-4} - 10^{-2}$ respectively. A summary of the baseline set of parameter values used in the computational simulations is given in the table below:

Parameter	**Description**	**Value**
D_1	cancer cell diffusion coefficient	0.00035
μ	cancer cell proliferation rate	0.15
γ	matrix degrading rate	8.15
D_3	MDE diffusion coefficient	0.00491
α	MDE production rate	0.75
λ	MDE degradation rate	0.5

Given that the main aim of the computational simulations was to examine the relative importance of cell-cell and cell-matrix adhesion, we varied the two parameters S_{11} and S_{12} over a range of values as follows:

Parameter	**Description**	**Value**
S_{11}	cell-cell adhesion coefficient	$0 - 0.5$
S_{12}	cell-matrix adhesion coefficient	$0 - 0.5$

We note that the parameter values given above have been taken from a number of different experiments and that many of the estimated parameters will have been measured in highly-controlled, laboratory conditions. Such experimental systems are very different from the actual *in vivo* biological system which evolves over time. However, we note that novel experimental assays now exist which are aimed at quantifying cancer cell invasion of tissue, both in 3-dimensional collagen gels and in mice[27,28]. In future, such experimental systems may help determine more accurately the actual *in vivo* parameter values.

4.3. *Simulation results*

All model simulations were performed using the MATLAB® system. The numerical scheme follows the method of lines by first discretising the non-local model in space, yielding an initial value problem for a large system of ordinary differential equations. This system is then solved using the time integration scheme ROWMAP[45], implemented in a Fortran subroutine and called from MATLAB®. For the discretisation in space we use a second-order finite volume approach which makes use of flux-limiting for an accurate discretisation of the taxis/adhesion term. A key to efficiency for the spatial discretisation of the non-local model is an accurate approximation of the non-local term and its efficient evaluation using FFT techniques. More details of the numerical scheme are outlined in Gerisch and Chaplain[19] and full details are given in Gerisch[20]. All our simulations were performed on a spatial domain $\Omega = (-4, 4)$, with periodic boundary conditions (in all the numerical experiments described below the boundary conditions had no or no significant effect on the solution). Initial conditions were the same for each simulation i.e. an initial mass of cancer cells was placed near the origin, having already released some MDE that had degraded the ECM i.e.

$$\begin{aligned} c(x,0) &= exp(-100x^2), \\ v(x,0) &= 1 - c(x,0), \\ m(x,0) &= 0.5c(x,0). \end{aligned}$$

Figure 1 shows the plots of the solution profiles of the cancer cell and ECM density and MDE concentration at times $t = 10, 20, 30, 40$ from a simulation of

the invasion model. In these simulations, the cell-cell adhesion parameter S_{11} has a value $S_{11} = 0.01$, while the cell-matrix adhesion parameter S_{12} takes the value $S_{12} = 0.02$. As can be seen from the plots, as time increases the cancer cells invade further into the matrix in the manner of a "standard" advancing front.

We now consider the effect of increasing the cell-matrix adhesion parameter S_{12}. Figure 2 shows the plots of the solution profiles of the cancer cell and ECM density and MDE concentration at times $t = 10, 20, 30, 40$ where the cell-cell adhesion parameter $S_{11} = 0.01$, while the cell-matrix adhesion parameter S_{12} has been increased and now takes the value $S_{12} = 0.5$. Once again, as can be seen from the plots, as time increases the cancer cells invade further into the matrix. However, in contrast to the cancer cell profiles of figure 1, the cancer cell profiles here are more heterogeneous. As time increases, behind the leading front of invading cells, cancer cell proliferation fills the gap created through degradation of the ECM.

Figure 3 shows the plots of the solution profiles of the cancer cell and ECM density and MDE concentration at times $t = 10, 20, 30, 40$ where the cell-cell adhesion parameter has been increased from its previous value of 0.01 and is now taken to be $S_{11} = 0.05$. The cell-matrix adhesion parameter S_{12} remains unchanged from the previous value $S_{12} = 0.5$. Once again, as can be seen from the plots, as time increases the cancer cells invade further into the matrix. However, the cancer cell profiles here are yet more heterogeneous than both the previous figures.

Next we consider the case where we have a large cell-cell adhesion value and a small cell-matrix adhesion value. Figure 4 shows the plots of the solution profiles of the cancer cell and ECM density and MDE concentration at times $t = 10, 20, 30, 40$ where the cell-cell adhesion parameter has been increased to be $S_{11} = 0.5$. The cell-matrix adhesion parameter S_{12} has been decreased to a value $S_{12} = 0.01$. As can be seen from the plots, as time increases the increased value of S_{11} prevents the cancer cells invading into the matrix. However a small fragment of cancer cells does "break off" from the main cancer cell mass which is localised near the origin, but because of the high cell-cell adhesion does not manage to penetrate deeply into the matrix and itself remains localised around $x = 0.3$.

In the next set of figures we consider a case where the cell-cell and cell-matrix adhesion parameters take an equal value of 0.1 i.e. $S_{11} = S_{12} = 0.1$. Figure 5 shows the plots of the solution profiles of the cancer cell and ECM density and MDE concentration at times $t = 10, 20, 30, 40$. As can be seen from the plots, as time increases a small fragment of cancer cells does "break off" from the main cancer cell mass localised near the origin, but this time manages to continue to invade the ECM as a localised mass, perhaps modelling the initiation of metastatic spread.

Finally we consider two scenarios where the parameters S_{11} and S_{12} are time-dependent in such as way as to model the effect of an increasingly malignant and aggressive invading cancer. It is known that as a cancer progresses and becomes more malignant, successive mutations cause a reduction in cell-cell adhesion and an increase in cell-matrix adhesion. Therefore we consider S_{11} to be a monotonic decreasing function of time and S_{12} a monotonic increasing function of time.

Figure 6 shows the plots of the solution profiles of the cancer cell and ECM density and MDE concentration at times $t = 10, 20, 30, 40$ where $S_{11} = 0.01 + 0.49\exp(-0.01t^2)$ (i.e. S_{11} decreases from a maximum value of 0.5 to 0.01) and $S_{12} = 0.2$. As can be seen from the plots, the cancer cells invade the ECM in a manner which consists of aspects from all the previous simulations.

Figure 7 shows the plots of the solution profiles of the cancer cell and ECM density and MDE concentration at times $t = 10, 20, 30, 40$ where $S_{11} = 0.01 + 0.49\exp(-0.01t^2)$ (i.e. S_{11} decreases from a maximum value of 0.5 to a minimum value of 0.01) and $S_{12} = 0.5 - 0.45\exp(-0.01t^2)$ (i.e. S_{12} increases from a minimum value of 0.05 to a maximum value of 0.5). As can be seen from the plots, the cancer cells invade the ECM in a manner in a more heterogeneous manner than in the previous figure.

Overall, the compuational simulation results show that a range of heterogeneous invasive behaviour can be observed by varying the two adhesion parameters S_{11} and S_{12}.

5. Discussion

In this paper we have developed a mathematical model of cancer cell invasion of tissue. The main focus of the paper was to examine the relative effects of cell-cell adhesion and cell-matrix adhesion on the invasion process. In order to achieve this, we formulated a minimal mathematical model using a system of nonlinear, non-local partial integro-differential equations describing the spatio-temporal dynamics of cancer cells, matrix degrading enzyme and extracellular matrix (tissue). Cell-cell adhesion and cell-matrix adhesion were modelled using non-local terms following the approach of Armstrong et al.[3] and Gerisch and Chaplain[19]. Certain analytical results were proved and computational results of numerical simulations of our system were given.

Having formulated our model in Sec. 3, in Sec. 4 we presented a mathematical analysis of our model and proved certain existence, uniqueness and smoothness results concerning the solutions of this system. First we proved the existence of local-in-time solutions using the Banach contraction mapping theorem and uniqueness of solutions using certain differential inequalities and Gronwall's Lemma. Finally, using Gronwall's Lemma and the Moser-Alikakos Method, we proved that our solution is bounded and global in time.

In Sec. 5, we presented the compuational results of numerical simulations of our model, in particular examining the relative effects of two key parameters of the model, S_{11} and S_{12}, the cell-cell adhesion coefficient and the cell-matrix adhesion coefficient, respectively. The computational simulation results showed a range of spatio-temporal behaviour depending on the relative sizes of S_{11} and S_{12}. These behaviours may be classified as follows:

(1) The cancer cells invade the tissue relatively slowly in a non-aggressive manner, with the extracellular matrix being degraded by the enzymes (see Fig. 1). This

occurs when both the cell-cell and cell-matrix adhesion are rela- tively small ($S_{11} = 0.01$ and $S_{12} = 0.01$) and represents the fact that the cancer cells have not developed strong enough cell-matrix adhesions and so remain rather localised;

(2) The cancer cells invade the tissue more quickly with a slightly more heterogeneous profile, again with the extracellular matrix being degraded by the enzymes (see Fig. 2). This occurs when the cell-cell adhesion is relatively small and the cell-matrix adhesion is relatively big ($S_{11} = 0.01$ and $S_{12} = 0.5$). This represents the fact that the cancer cells have developed stronger cell-matrix adhesions and have become more aggressive;

(3) The cancer cells invade the tissue quickly with a highly heterogeneous profile (see Fig. 3). This occurs for a slightly increased value of the cell-cell adhesion (compared with Figs. 1,2) and a relatively large value of cell-matrix adhesion ($S_{11} = 0.05$ and $S_{12} = 0.5$).

(4) The invasion is almost stopped and the cancer cells remain localised around their initial conditions; the tissue is slowly degraded by the enzymes (see Fig. 4). This occurs for a large value of the cell-cell adhesion parameter and small value of the cell-matrix adhesion parameter ($S_{11} = 0.5$ and $S_{12} = 0.01$) and represents the situation where the cancer cells have not been able to break their strong cell-cell adhesion bounds and therefore are not able to invade efficiently;

(5) An invasive fragment of cancer cells breaks away from the central mass and invades in a metastatic manner (Fig. 5). This occurs when the cell-cell and cell-matrix adhesion parameters are equal but relatively strong ($S_{11} = 0.1$, $S_{12} = 0.1$);

(6) A combination of these effects is obtained by varying the parameters S_{11} and S_{12} with time (Figs. 6,7), which is generally the case during cancer development and models the tendency of a cancer to become increasingly malignant and aggressive over time.

In general the results from the computational simulations show that an increased value of the cell-cell adhesion parameter results in a more heterogenous pattern of invasion whereas an increased value of the cell-matrix adhesion parameter results in a faster invasion. These results are in qualitative agreement with previous studies and models[6,7,15,25]. The scenario that probably reflects the biological reality the best is where the cell-cell and cell-matrix adhesion parameters change dynamically over time (Figs. 6,7). Therefore experiments which could precisely measure these effects would be useful to aid in understanding the malignant progression of a cancer[27,28].

Future work may consider developing a multiscale version the current model. It is clear that events at the sub-cellular and cellular level influence events at the tissue scale, which is where the focus of the current paper lies. We could therefore aim to extend the current model by adopting the approach of Marciniak-Czochra & Ptashnyk[26] and try to incorporate sub-cellular and cellular information (e.g. data concerning E-cadherin, β-catenin levels[33,34]) into our cell-cell adhesion parameter

S_{11}. Using this modelling approach it would also be possible to incorporate data concerning interactions between integrins (on the cell surface) and extracellular matrix components into the cell-matrix adhesion parameter S_{12}.

Acknowledgment:
Z.S. and M.L. would like to thank the Polish Ministry of Science and Higher Education for a financial support under the grant N N201 362536. The work of Z.S. was also partially supported by the Polish-German PhD studies Graduate College "Complex Processes: Modelling, Simulation and Optimization". The work of D.W. was supported by the Polish Ministry of Science and Higher Education for a financial support under the grant N N201547638. The work of M.A.J.C. was supported by an ERC Advanced Investigator Grant, No. 227619, "From mutations to metastases: Multiscale mathematical modelling of cancer growth and spread".

References

1. A.R.A. Anderson, M.A.J. Chaplain, E.L. Newman, R.J.C. Steele, and A.M. Thompson, Mathematical modelling of tumour invasion and metastasis, *J. Theor. Med.* **2** (2000) 129–154.
2. A.R.A. Anderson, A hybrid mathematical model of solid tumour invasion: The importance of cell adhesion, *Math. Med. Biol.* **22** (2005) 163–186.
3. N.J. Armstrong, K.J. Painter, J.A. Sherratt, A continuum approach to modelling cell-cell adhesion, *J. Theor. Biol.* **243** (2006) 98–113.
4. N. Bellomo, N.K. Li and P.K. Maini, On the foundations of cancer modelling: Selected topics, speculations, and perspectives, *Math. Mod. Meth. Appl. Sci.* **18** (2008) 593–646.
5. D. Bray, *Cell Movements: From Molecules to Motility* (Garland Publishing, 2000).
6. H.M. Byrne and M.A.J. Chaplain, Modelling the role of cell-cell adhesion in the growth and development of carcinomas *Math. Comput. Modelling* **24** (1996) 1–17.
7. H.M. Byrne and M.A.J. Chaplain, Free boundary value problems associated with the growth and development of multicellular spheroids, *Euro. Jnl. of Applied Mathematics* **8** (1997) 639–658.
8. H.M. Byrne, M.A.J. Chaplain, G.J. Pettet, and D.L.S. McElwain, A mathematical model of trophoblast invasion, *J. Theor. Med.* **1** (1998) 275–286.
9. M.A.J. Chaplain and B.D. Sleeman, Modelling the growth of solid tumours and incorporating a method for their classification using nonfinear elasticity theory, *J. Math. Biol.* **31** (1991) 431–473.
10. M.A.J. Chaplain and G. Lolas, Mathematical modelling of cancer cell invasion of tissue: The role of the urokinase plasminogen activation system, *Math. Mod. Meth. Appl. Sci.* **15** (2005) 1685–1734.
11. M.A.J. Chaplain and G. Lolas. Mathematical modelling of cancer invasion of tissue: Dynamic heterogeneity, *Net. Hetero. Med.* **1** (2006) 399–439.
12. J.W. Cholewa and T. Dlotko, *Global Attractors in Abstract Parabolic Problems* (Cambridge University Press, Cambridge, 2000).
13. A. De Pablo and J. L. Vázquez, Travelling waves and finite propagation in a reaction-diffusion equation, *J. Diff. Eq.* **93** (1991) 19 – 61.
14. F. Filbet, P. Laurençot and B. Perthame, Derivation of hyperbolic models for chemosensitive movement, *J. Math. Biol.* **50** (2005) 189 – 207.

15. H.B. Frieboes, X. Zheng, C-H. Sun, B. Tromberg, R.A. Gatenby and V. Cristini, An integrated computational/experimental model of tumor invasion, *Cancer Res.* **66** (2006) 1597–1604.
16. P. Friedl and K. Wolf, Tumour-cell invasion and migration: Diversity and escape mechanisms, *Nature Rev. Cancer* **3** (2003) 362–374.
17. R.A. Gatenby and E.T. Gawlinski, A reaction-diffusion model of cancer invasion, *Cancer Res.* **56** (1996) 5745–5753.
18. R.A. Gatenby, E.T. Gawlinski, A.F. Gmitro, B. Kaylor and R.J. Gillies, Acid-mediated tumor invasion: a multidisciplinary study, *Cancer Res.* **66** (2006) 5216–5223.
19. A. Gerisch and M.A.J. Chaplain, Mathematical modelling of cancer cell invasion of tissue: Local and non-local models and the effect of adhesion, *J. Theor. Biol.* **250** (2008) 684–704.
20. A. Gerisch, On the approximation and efficient evaluation of integral terms in PDE models of cell adhesion, *IMA J. Numer. Anal.* doi: 10.1093/imanum/drp027 (2009).
21. D. Hanahan and R.A. Weinberg, The hallmarks of cancer, *Cell* **100** (2000) 57–70.
22. D.Henry, *Geometric theory of semilinear parabolic equations* (Lecture Notes Math. 840. Springer-Verlag, Berlin, New York, 1981).
23. M. Lachowicz, Micro and meso scales of description corresponding to a model of tissue invasion by solid tumours, *Math. Mod. Meth. Appl. Sci.* **15** (2005) 1667–1683.
24. L.A. Liotta and E.C. Kohn, The microenvironment of the tumour-host interface, *Nature* **411** (2001) 375–379.
25. P. Macklin and J.S. Lowengrub, Nonlinear simulation of the effect of microenvironment on tumor growth, *J. Theor. Biol.* **254** (2007) 677–704.
26. A. Marciniak-Czochra and M. Ptashnyk, Derivation of a macroscopic receptor-based model using homogenization techniques, *SIAM J. Appl. Math. Anal.* **40** (2008) 215–237.
27. V.L. Martins, J.J. Vyas, M. Chen, K. Purdie, C.A. Mein, A.P. South, A. Storey, J.A. McGrath and E.A. O'Toole, Increased invasive behaviour in cutaneous squamous cell carcinoma with loss of basement-membrane type VII collagen, *J. Cell Sci.* **122** (2009) 1788–1799.
28. M.L. Nyström, G.J. Thomas, M. Stone, I.C. Mackenzie, I.R. Hart and J.F. Marshall, Development of a quantitative method to analyse tumour cell invasion in organotypic culture, *J. Pathol.* **205** (2005) 468–475.
29. J.T. Oden, A. Hawkins and S. Prudhomme, General Diffuse-Interface Theories and an Approach to Predictive Tumor Growth Modeling, *Math. Models Method Appl. Sci.* **20** (2010) 477–517.
30. M.E. Orme and M.A.J. Chaplain, Two-dimensional models of tumour angiogenesis and anti-angiogenesis strategies, *IMA J. Math. Appl. Med. Biol.* **14** (1997) 189–205.
31. A.J. Perumpanani, J.A. Sherratt, J. Norbury, and H.M. Byrne, Biological inferences from a mathematical model for malignant invasion, *Invasion & Metastasis* **16** (1996) 209–221.
32. A.J. Perumpanani, D.L. Simmons, A.J.H. Gearing, K.M. Miller, G. Ward, J. Norbury, M. Schneemann, and J.A. Sherratt, Extracellular matrix-mediated chemotaxis can impede cell migration, *Proc. Roy. Soc. London, Ser. B* **265** (1998) 2347–2352.
33. I. Ramis Conde, D. Drasdo, M..A.J. Chaplain and A.R.A. Anderson, Modelling the influence of the E-Cadherin - β-Catenin pathway in cancer cell invasion and tissue architecture: A multi-scale approach, *Biophys. J.* (2008) **95** 155–165.
34. I. Ramis-Conde, M.A.J. Chaplain, A.R.A. Anderson and D. Drasdo, Multi-scale modelling of cancer cell intravasation: the role of cadherins in metastasis, *Phys. Biol.* **6** 016008 (2009) (12pp).

35. T. Runst and W. Stickel, *Sobolev Spaces of Fractional Order, Nemytskij Operators and Nonlinear Partial Differential Equations,* (Walter de Gruyter, Berlin, 1996).
36. F. Sánchez-Garduño and P.K. Maini, Existence and uniqueness of a sharp travelling wave in degenerate non-linear diffusion Fisher-KPP equation, *J. Math. Biol.* **33** (1994) 163 – 192.
37. F. Sánchez-Garduño and P.K. Maini, Travelling wave phenomena in some degenerate reaction-diffusion equations, *J. Diff. Eq.* **117** (1995) 281 – 319.
38. J.A. Sherratt, S.A. Gourley, N.J. Armstrong and K.J. Painter, Boundedness of solutions of a non-local reaction-diffusion model for adhesion in cell aggregation and cancer invasion, *Euro. Jnl. of Applied Mathematics* **20** (2009) 123–144.
39. M.B. Sporn, The war on cancer, *Lancet* **347** (1996) 1377–1381.
40. Z. Szymańska, J. Urbański and A. Marciniak-Czochra, Mathematical modelling of the influence of heat shock proteins on cancer invasion of tissue, *J. Math. Biol.* **58** (2009) 819–844.
41. Z. Szymańska, C. Morales Rodrigo, M. Lachowicz and M.A.J. Chaplain, Mathematical modelling of cancer invasion of tissue: the role and effect of nonlocal interactions, *Math. Mod. Meth. Appl. Sci.* **19** (2009) 157–281.
42. H.Triebel, *Interpolation Theory, Function Spaces, Differential Operators* (Veb Deutscher, Berlin, 1978).
43. H.Triebel, *Theory of Function Spaces* (Birkhauser, Basel, 1983).
44. R.A. Weinberg, *The Biology of Cancer* (Garland Science, 2007).
45. R. Weiner, B.A. Schmitt, and H. Podhaisky, ROWMAP—a ROW-code with Krylov techniques for large stiff ODEs, *Appl. Numer. Math.* **25** (1997) 303–319.
46. M.H. Zaman, L.M. Trapani, A.L. Sieminski, D. Mackellar, H. Gong, R.D. Kamm, A. Wells, D.A. Lauffenburger and P. Matsudaira, Migration of tumor cells in 3D matrices is governed by matrix stiffness along with cell-matrix adhesion and proteolysis, *PNAS* **103**, (2006) 10889 – 10894.

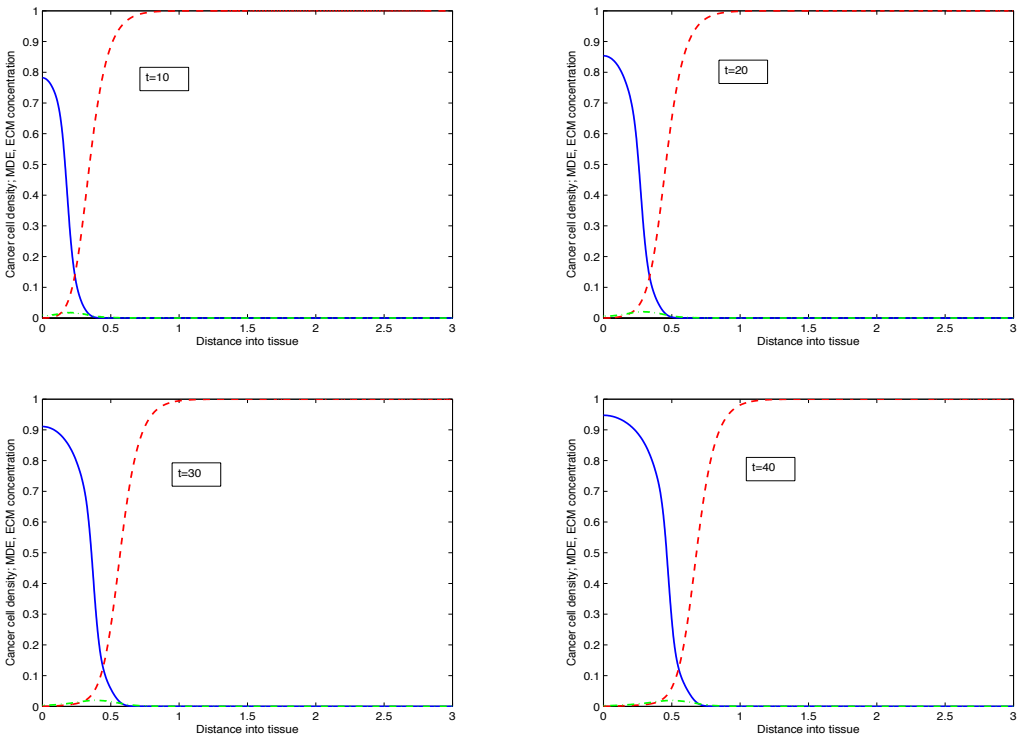

Fig. 1. Plots showing the solution profiles of the cancer cell (blue) and ECM density (red) and MDE concentration (green) at times $t = 10, 20, 30, 40$ from a simulation of the invasion model. The cell-cell adhesion parameter is $S_{11} = 0.01$, while the cell-matrix adhesion parameter $S_{12} = 0.02$. The plots show that as time increases the cancer cells invade the ECM more deeply.

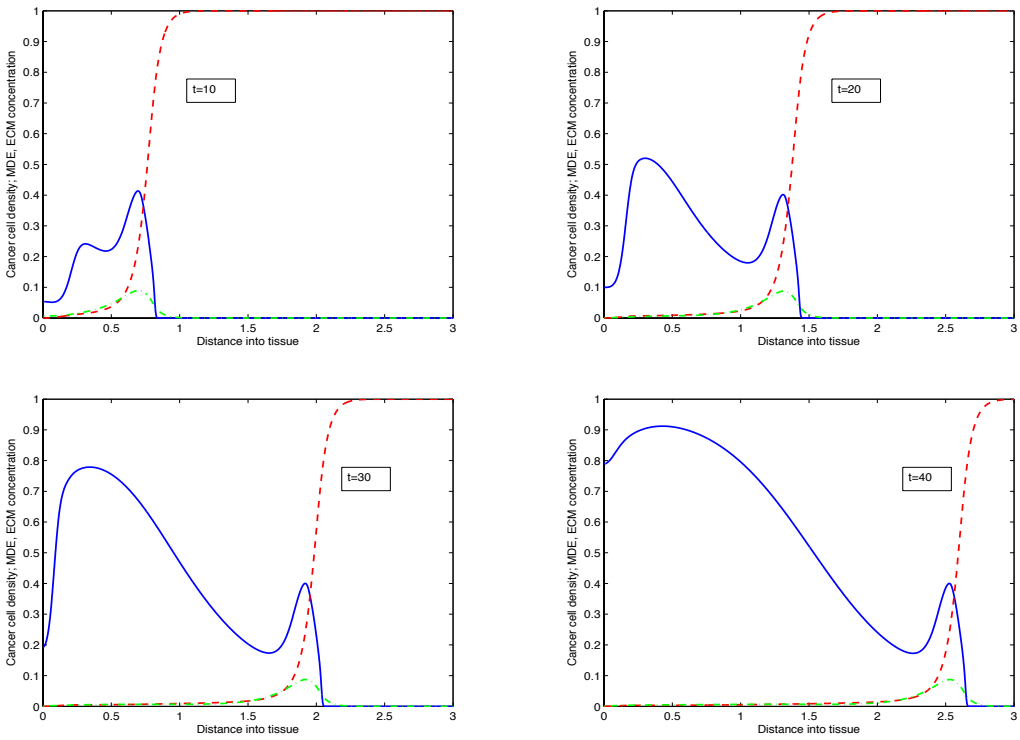

Fig. 2. Plots showing the solution profiles of the cancer cell (blue) and ECM density (red) and MDE concentration (green) at times $t = 10, 20, 30, 40$ from a simulation of the invasion model. The cell-cell adhesion parameter is $S_{11} = 0.01$, while the cell-matrix adhesion parameter $S_{12} = 0.5$. The plots show that as time increases the cancer cells invade the ECM more deeply but with a different profile than those in figure 1.

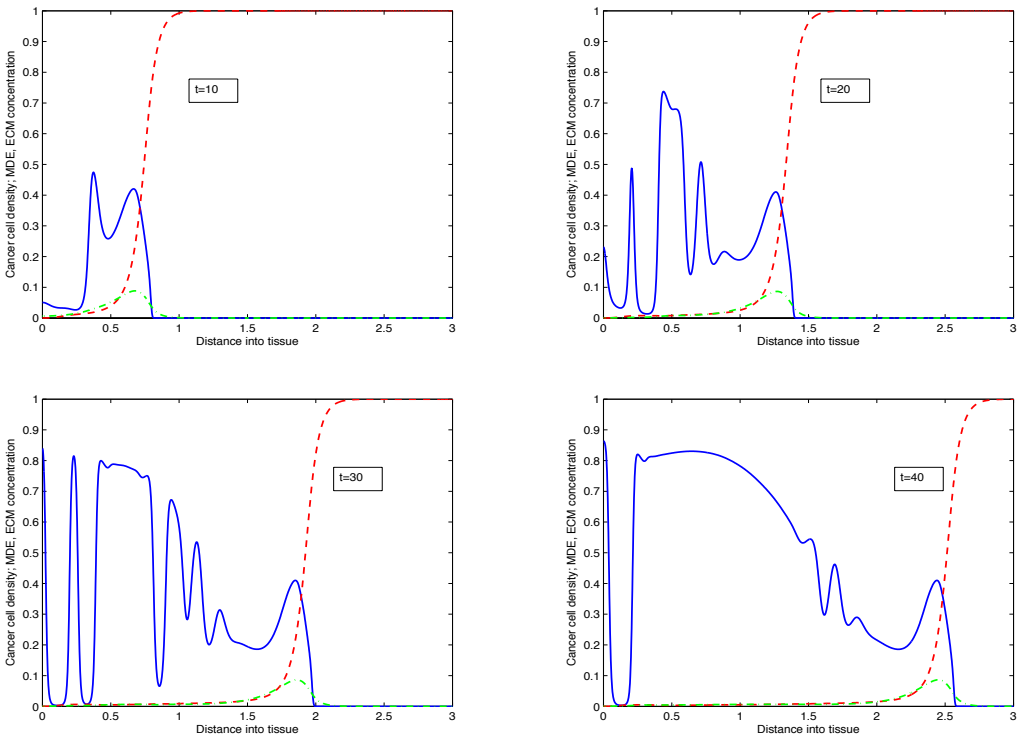

Fig. 3. Plots showing the solution profiles of the cancer cell (blue) and ECM density (red) and MDE concentration (green) at times $t = 10, 20, 30, 40$ from a simulation of the invasion model. The cell-cell adhesion parameter is $S_{11} = 0.05$, while the cell-matrix adhesion parameter $S_{12} = 0.5$. The plots show that as time increases the cancer cells invade the ECM more deeply but with a more heterogeneous profile than those in figures 1 and 2.

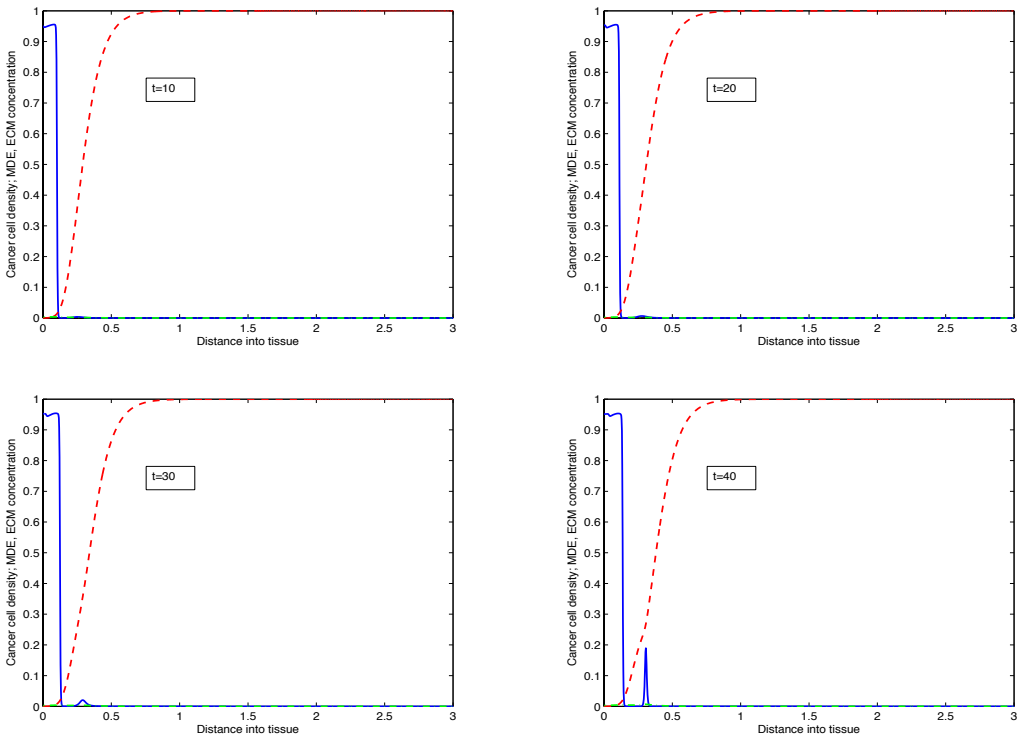

Fig. 4. Plots showing the solution profiles of the cancer cell (blue) and ECM density (red) and MDE concentration (green) at times $t = 10, 20, 30, 40$ from a simulation of the invasion model. The cell-cell adhesion parameter is $S_{11} = 0.5$, while the cell-matrix adhesion parameter $S_{12} = 0.01$. The plots show that because of the increased cell-cell adhesion, the cancer cells remain localised around the origin, although a fragment of cells breaks away from the main mass but then itself remains localised around $x = 0.3$.

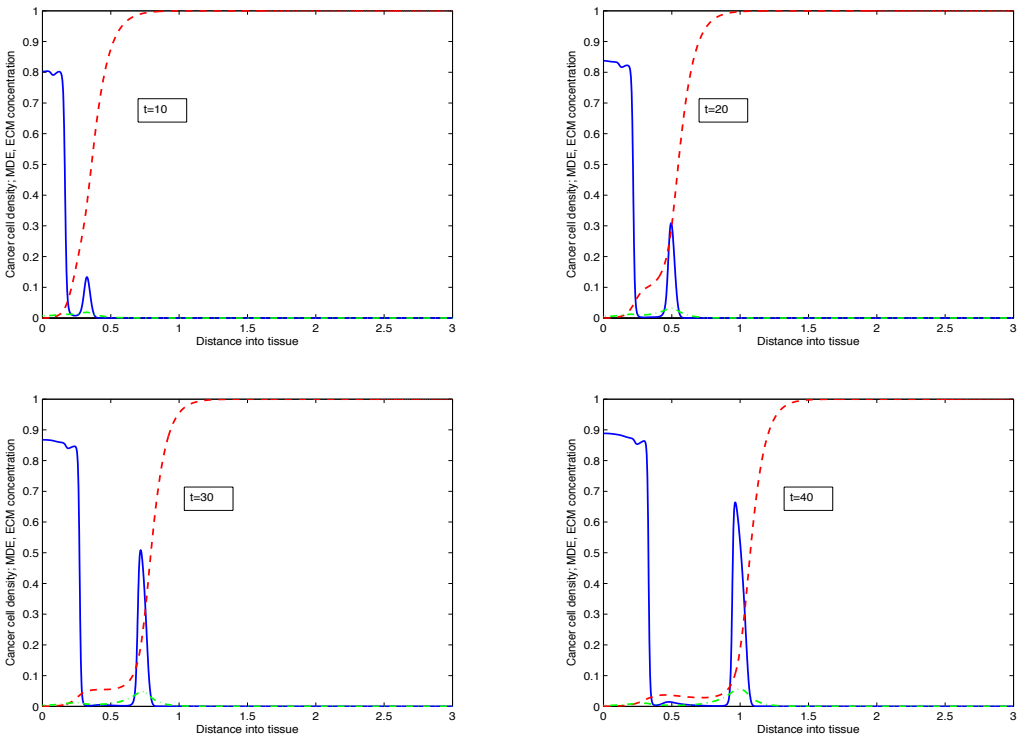

Fig. 5. Plots showing the solution profiles of the cancer cell (blue) and ECM density (red) and MDE concentration (green) at times $t = 10, 20, 30, 40$ from a simulation of the invasion model. The cell-cell adhesion parameter is $S_{11} = 0.1$, while the cell-matrix adhesion parameter $S_{12} = 0.1$. The plots show an invasive fragment of cancer cells breaking away from the central mass and invading in a localised "metastatic" manner.

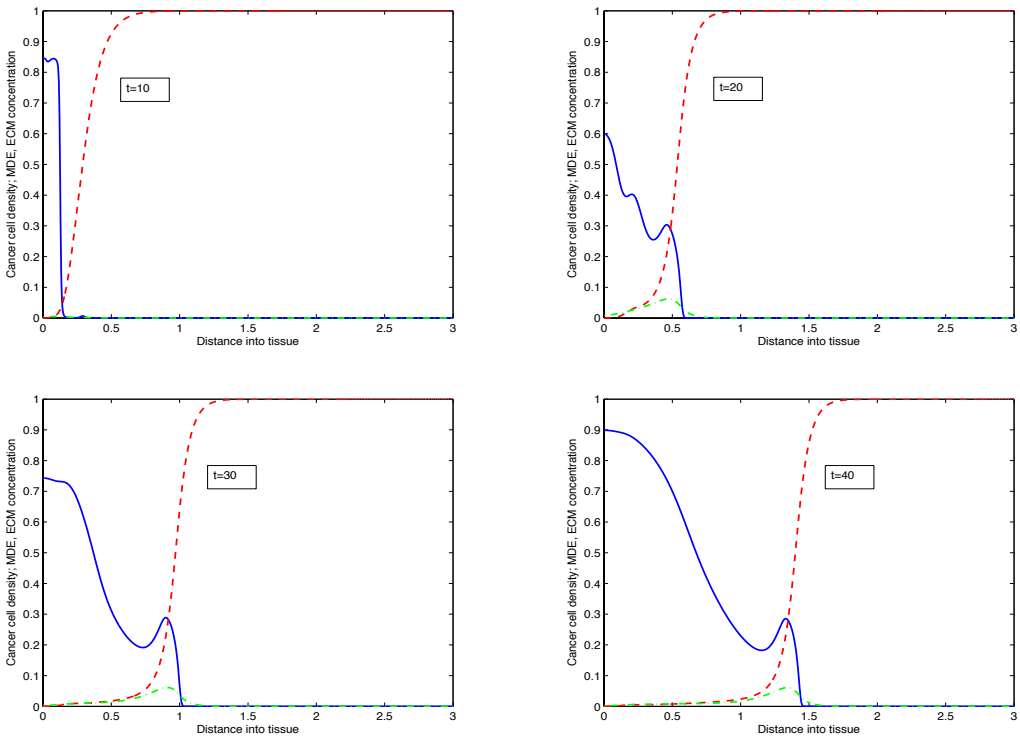

Fig. 6. Plots showing the solution profiles of the cancer cell (blue) and ECM density (red) and MDE concentration (green) at times $t = 10, 20, 30, 40$ from a simulation of the invasion model. The cell-cell adhesion parameter S_{11} is a monotonic decreasing function of time (see text for precise functional form), while $S_{12} = 0.2$. The cancer cells invade in a manner combining aspects of the previous invasive plots.

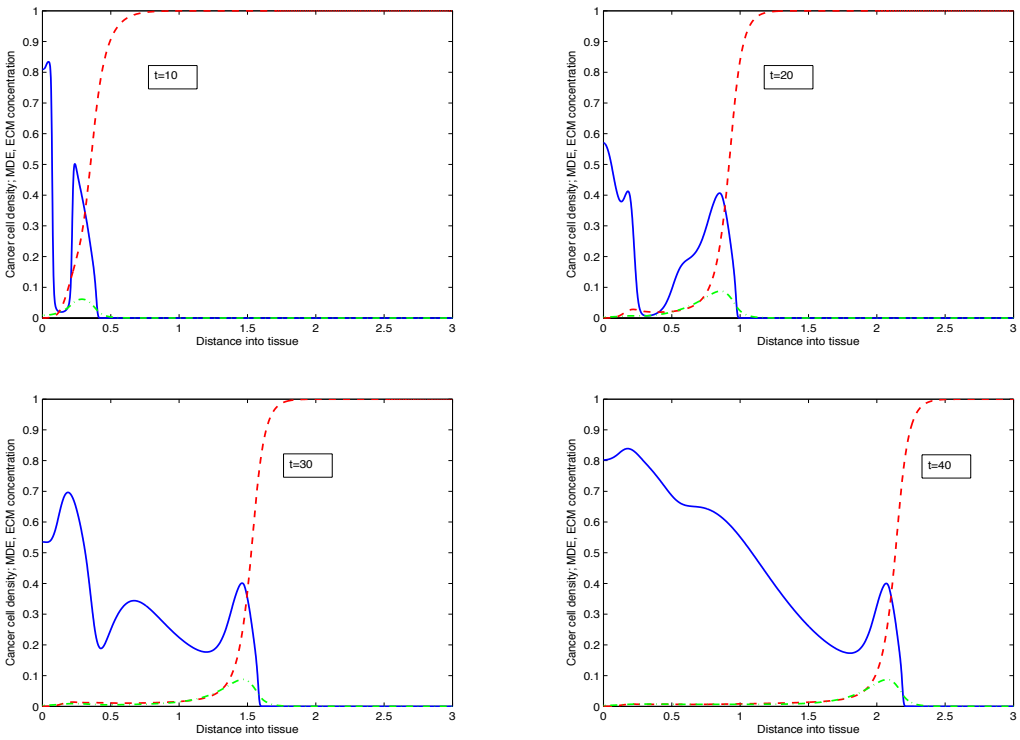

Fig. 7. Plots showing the solution profiles of the cancer cell (blue) and ECM density (red) and MDE concentration (green) at times $t = 10, 20, 30, 40$ from a simulation of the invasion model. The cell-cell adhesion parameter S_{11} is a monotonic decreasing function of time, while the cell-matrix adhesion parameter S_{12} is a monotonic increasing function of time (see text for precise functional forms). The cancer cells invade in a manner combining aspects of the previous invasive plots seen in Figures 1 - 5, but more heterogeneously than Figure 6.